Article

J. Biol. Regul. Homeost. Agents. 2023; 37(12): 6501–6510
https://doi.org/10.23812/j.biol.regul.homeost.agents.20233712.615

Osteopontin as a Biomarker for Early Diagnosis of Renal Damage during Experimental Metabolic Syndrome

Ramona D'Amico[1], Rosalba Siracusa[1], Marika Cordaro[2], Roberta Fusco[1], Alessia Arangia[1], Livia Interdonato[1], Ylenia Marino[1], Gianluca Antonio Franco[3], Salvatore Cuzzocrea[1], Rosanna Di Paola[3,*], Daniela Impellizzeri[1]

[1]Department of Chemical, Biological, Pharmaceutical and Environmental Sciences, University of Messina, 98166 Messina, Italy
[2]Department of Biomedical, Dental and Morphological and Functional Imaging, University of Messina, 98125 Messina, Italy
[3]Department of Veterinary Science, University of Messina, 98168 Messina, Italy
*Correspondence: dipaolar@unime.it (Rosanna Di Paola)
Published: 20 December 2023

Background: Excess consumption of fructose is a significant factor in the development of metabolic syndrome (MetS). It may also play a role in the progress of chronic kidney disease (CKD). Osteopontin (OPN) is a pleiotropic, multi-phosphorylated glycoprotein which plays important roles in diseases as well as in a wide range of biological activities. Based on these findings, the aim of this study was to evaluate OPN as a biomarker for the early detection of renal injury during an experimental model of fructose associated MetS in mice.
Methods: Male CD1 mice aged 8–10 weeks were used. Fructose mice were given 30% fructose solution in drinking water, while control mice were given normal drinking water for 56 days. At sacrifice, kidneys, blood and urine of mice were collected. Biochemical, histological (hematoxylin and eosin and Masson's trichrome), immunohistochemical and molecular analyses (western blot, real-time quantitative polymerase chain reaction (RT-qPCR)) were performed.
Results: Compared to controls, Fructose mice showed increased levels of glucose, total cholesterol (TC), triglyceride (TG), low-density lipoprotein (LDL), alanine aminotransferase (ALT), and aspartate aminotransferase (AST), as well as creatinine and blood urea nitrogen (BUN). In addition, significant histological kidney injury and fibrosis were observed in Fructose mice. These alterations were associated with increased levels of plasma and renal tissue OPN.
Conclusions: Thus, new biomarkers such as OPN can be clinically useful to help predict kidney damage in MetS.

Keywords: metabolic syndrome; fructose; osteopontin; kidney injury; biomarker

Introduction

Fructose (FR) is a natural monosaccharide found in fruits and honey. Its consumption has been rising sharply around the globe, largely as a result of the addition of high-fructose corn syrup (HFCS) and sucrose, a disaccharide composed of 50% fructose and 50% glucose, to foods and soft drinks. Excessive fructose consumption is a major factor in the increased prevalence of metabolic syndrome (MetS) [1]. MetS is a recognized risk factor for increased mortality, cardiovascular disease, and type 2 diabetes. MetS may also contribute to chronic kidney disease (CKD) [2]. It has been proposed that consuming too much fructose may be a cause of both MetS and CKD [2].

It has been found in rats that eating a diet high in fructose is a risk factor for MetS, proximal tubule injury and urolithiasis [3]. Mice with MetS develop not only CKD but also sarcopenia and reduce lifespan [4]. Thus, a better understanding of how a high fructose diet causes MetS and why it is linked to CKD is clinically important. With distinct metabolic problems manifesting at various stages, MetS is a progressive illness which includes a variety of ailments. These abnormalities can be detected and monitored via serum biomarkers. Biomarkers searched included adipokines, neuropeptides, pro-inflammatory and anti-inflammatory cytokines, markers of antioxidant status and prothrombic factors [5]. In order to effectively treat those who already have MetS and reduce its overall prevalence in the general population, it would be extremely beneficial to identify biomarkers which could be used clinically to predict and establish a diagnosis of MetS.

Osteopontin (OPN) is a secreted, pleiotropic, multi-phosphorylated glycoprotein, first recognized as secreted phosphoprotein 1 (SPP1) [6]. Though it was originally found in bone, subsequent research revealed that it is expressed in multiple tissues [7]. OPN plays important roles in diseases such as chronic inflammation and tumors, as well as in a wide range of biological activities, including biomineralization and physiological processes involved in cellular homeostasis [8,9]. OPN, also known as bone sialoprotein 1 and early T-lymphocyte activation 1 protein [10], activates a variety of immune cells, including T-cells, B-

Journal of
BIOLOGICAL REGULATORS
and Homeostatic Agents

cells, macrophages, natural killer cells, and Kupffer cells [11]. OPN is categorized as a small integrin-binding ligand N-linked glycoprotein family member [12] which modulates cell and matrix signaling, cooperating with integrins and CD44 receptors [10]. Its highest concentration among all tissues is found in the kidney [13]. Within the kidney, OPN is principally expressed in the loop of Henle and nephrons [6], but after kidney injury, its level is also upregulated in glomeruli and tubular segments [6]. Thus, it is not unexpected that OPN is involved in numerous kidney diseases [14]. OPN deficiency guards the kidneys against aldosterone-induced inflammation, oxidative stress, and interstitial fibrosis [15]. Previous results also indicated that OPN expressed by tubular epithelial cells is an important element in inflammatory responses which involve natural killer (NK) cell activity in kidney disease [16].

Based on this, it's needed to find new biomarkers by using a mouse model of MetS and explore biomarkers which could be used for monitoring the effects of excessive fructose intake. The aim of this study was to test OPN as a biomarker for kidney damage in experimental MetS induced by the consumption of 30% fructose solution in mice for 56 days through biochemical, histological, immunohistochemical and molecular analyses.

Materials and Methods

Animals

CD1 male mice (8–10 weeks of age, 22–25 gr; Envigo, Milan, Italy), were used. Mice were housed in individual plexigass cages (42 × 34 × 17 cm) under conditions of optimum light, temperature, and humidity (12:12 light-dark cycle at 21 ± 1 °C and 50 ± 5% humidity) and acclimated for 1 week. The animals were fed with traditional diet (Envigo, Milan IT, 2018 Global rodent diet, Teklad, T.2018MI.12). This study was authorized by the University of Messina Review Board for the care of animals. Animal care conformed to the new legislation for the safety of animals used for scientific commitments (Italian D. Lgs. 2014/26 and EU Directive 2010/63). Ethical code: n.897/2021-PR.

Metabolic Syndrome Induction

Fructose mice were given 30% fructose (F0-127, Sigma-Aldrich, St., Louis, MO, USA) solution (30 gr of fructose dissolved in 100 mL of tap water) every day for 56 days. This solution was the drinking water of Fructose mice. Control mice were given only tap water for 56 days [17]. Body weight was checked throughout the experiment two times a week by (accuracy 0.1 g–4000 g, Instrument KERN 440-49N, Biogenerica, Catania, Italy). Kidneys, blood and urine were collected at the end of experiment (at 56th day). Whole blood samples were collected by deeply anesthetized mice with 1–2% isoflurane in 100% O_2 (Harvard Apparatus K016522, Fluovac, Edenbridge, UK) by a cardiac puncture (quantity of blood obtained 1 mL) and centrifuged for 15 min at 4 °C at 3000 g to separate serum. Whole blood was also collected in tubes using Ethylenediaminetetraacetic acid (EDTA) as an anticoagulant and immediately centrifuged for 15 minutes at 3000 ×g at 2–8 °C to yield plasma. Plasma and serum were stored in a –80 °C freezer for next analyses. Urine (24 h) was collected near the end of the study (56th day) in mouse metabolic cages. The animals were sacrificed by overdose of anesthesia and cervical dislocation.

After being weighed at necropsy, the right kidneys were collected for histologic examination in 10% formalin tubes and the left kidneys were placed directly into liquid nitrogen following removal from the mouse and then were stored in a –80 °C freezer for western blot analyses and biochemical estimations.

Experimental Groups

Mice were randomly divided into two groups of $n = 6$:

- Control group (Sham): mice were supplied normal drinking water for 56 days;
- Fructose group (Fru): mice drank 30% fructose in drinking water for 56 days.

Glucose Tolerance Test (GTT)

After 56 days, all mice were fasted for 8 h and then received an injection of glucose (2 g/kg b.w., i.p.) [18]. Blood glucose was monitored at 0, 15, 60, and 120 min after glucose injection on blood samples collected from the tip of the tail vein, using a glucometer (3021858, Accu-Check, Roche, Monza, Italy). After the GTT, euthanasia was conducted by overdose of anesthesia (5% isoflurane, s3332l13a, Piramal Critical Care, Voorschoten, Netherlands) and cervical dislocation.

Evaluation of Clinical Biochemical Parameters

After sacrifice, whole blood samples were collected and centrifuged for 15 min at 4 °C at 3000 g to separate serum. Serum glucose, lipid profile, including the levels of total cholesterol (TC, 11506), total triglyceride (TG, 11529), low-density lipoprotein cholesterol (LDL-C, 11585), alanine aminotransferase (ALT, 11533), and aspartate aminotransferase (AST, 11531) were determined by using commercial kits according to the manufacturer's instructions, respectively (Biosystems, Reagents and Instruments, Barcelona, ES).

Plasma creatinine was determined by an enzymatic assay kit (80350, Mouse Creatinine Assay, Crystal Chem, Grove, IL, USA) and blood urea nitrogen (BUN) by (DIUR-100, Bioassay Systems, Hayward, CA, USA) kit. Twenty-four hour urinary creatinine was determined by an assay kit (500701, Cayman Chemical, Ann Arbor, MI, USA).

Food and Water Intake Measurements

Daily food and water intake was measured by subtracting the amount of food or water remaining in the cage or

water bottle. Specifically, we calculated the difference between the initial amount of food (30 gr) or water (30 mL) and the amount of food remaining in the cage or the remaining water present in the bottle. The food was weighed by (Instrument KERN 440-49N, accuracy 0.1 g–4000 g). The water consumption was measured by a graduated cylinder. The average daily food and water intake per mouse during each week was reported.

Histological Analysis

The right kidneys were dissected free from the abdominal aorta intact and fixed in formalin for 24 h after sacrifice. The fixed samples were then dehydrated by graded ethanols, embedded in paraffin and sectioned into 7-µm slices. The sections were attached to glass slides, then deparaffinized with xylene, stained with haematoxylin and eosin (H&E) (23109 and 23081, Bioptica, Milan, Italy) and observed under a Leica DM6 microscope (Leica Microsystems SpA, Milan, Italy) equipped with Leica LAS X Navigator software (3.4.2.1836.8.1.2, Leica Microsystems SpA, Milan, Italy).

Renal histopathological score was based on the histopathological appearance of the renal corpuscle (glomerulosclerosis, glomerular necrosis, Bowman's space dilation), renal tubules (dilation, coagulative necrosis, cloudy swelling, and fat droplet deposition), and the interstitium (congestion and mononuclear cells infiltration). The score grades were 0 (no lesion), 1 (mild damage), 2 (moderate damage), and 3 (high damage) [19].

To determine the degree of collagen fiber accumulation, a kidney section was stained with Masson's trichrome (21221, Bioptica, Milan, Italy). Three fields in different sections were randomly selected, and Masson's trichrome-stained area (blue) and total tissue area were determined. Their ratio was calculated as interstitial collagen deposit (fibrosis) [20].

Plasma Levels of OPN

Whole blood was collected at sacrifice in tubes using EDTA as an anticoagulant and immediately centrifuged for 15 minutes at 3000 ×g at 2–8 °C to yield plasma. A commercially available ELISA kit was used to determine plasma concentration of OPN (P10923.1, Biogenerica SRL, Catania, Italy).

Immunohistochemical Analyses

Immunohistochemical analyses were performed on right kidney sections as described [21–24]. Endogenous peroxidase in deparaffinized 7-µm thick sections was quenched with 0.3% H_2O_2 in methanol for 30 min. The sections were permeabilized with 0.1% Triton X-100 in phosphate buffered saline (PBS) for 20 min. Non-specific adsorption was minimized by incubating sections in 2% normal horse serum in phosphate buffered saline for 20 min. Endogenous biotin or avidin binding sites were blocked by sequential incubation for 15 min with avidin and biotin. The following primary antibodies were used: anti-Alpha Smooth Muscle Actin (α-SMA) antibody (1:100, sc-53015, Santa Cruz Biotechnology SCB, Biogenerica SRL, Catania, Italy) and Transforming Growth Factor (TGF)-β (1:100, sc-130348, SCB, Biogenerica SRL, Catania, Italy). Controls included buffer alone or non-specific purified rabbit IgG. Sections were cleaned with PBS and incubated with secondary antibody. Specific labeling was detected with a biotin-conjugated goat anti-rabbit IgG and 3,3′-Diaminobenzidine (DAB). Counterstain was developed with DAB (brown color) and eosin. A positive staining (brown color) was found in the sections, indicating that the immunoreactions were positive. Stained sections were observed using a Leica DM6 microscope (Leica Microsystems SpA, Milan, Italy). The histogram profile is related to the positive pixel intensity value obtained [21].

Real-Time Quantitative Polymerase Chain Reaction (RT-qPCR)

Total RNA was isolated from kidneys using RNeasy Mini Kit (74104, Qiagen, Milan, Italy) according to manufacturer's protocols. RNA was then quantified using a Nanodrop Spectrometer and subsequently used for cDNA synthesis using iScript RT-PCR kit (1708840, Bio-Rad, Milan, Italy). OPN mRNA was measured by RT-qPCR according to the manufacturer's instructions on a BioRad CFX Connect RT-qPCR machine using SYBR Green master mix and PrimePCRTM SYBR® Green Assay (BioRad) kit (169025678, BioRad, Milan, Italy). Each sample was normalized to the glyceraldehyde-3-phosphate dehydrogenase (GAPDH) mRNA expression (qt00199388, Biogenerica SRL, Catania, Italy).

Primers used:

for *OPN* (sense TACGACCATGAGATTGGCAGTGA, antisense TATAGGATCTGGGTGCAGGCTGTAA);

for *GAPDH* (sense TGTGTCCGTGGATCTGA, antisense TTGCTGTTGAAGTCGCAGGAG).

Western Blot

Western blots were performed as described [25–27]. Left kidney tissues (100 mg) from each mouse were suspended in extraction buffer A containing protease inhibitors cocktail (p8340, Sigma Aldrich, St., Louis, MO, USA) and Trizma® hydrochloride (Tris-HCl) (t5941, Sigma Aldrich, St., Louis, MO, USA), pH 7.4; 1 mM Ethylene glycol bis (2-aminoethyl ether) N,N,N′,N′-tetraacetic acid (EGTA) (e0396, Sigma Aldrich, St., Louis, MO, USA); 1 mM EDTA (bccd7594, Sigma Aldrich, St., Louis, MO, USA); sodium azide 100 mM NaN3 (S2002, Sigma Aldrich, St., Louis, MO, USA) beta-mercaptoethanol (m3148, Sigma Aldrich, St., Louis, MO, USA) Sodium fluoride 100 mM NAF (s7920, Sigma Aldrich, St., Louis, MO, USA), sucrose (s7903, Sigma Aldrich, St., Louis, MO, USA) and ho-

Journal of
BIOLOGICAL REGULATORS
and Homeostatic Agents

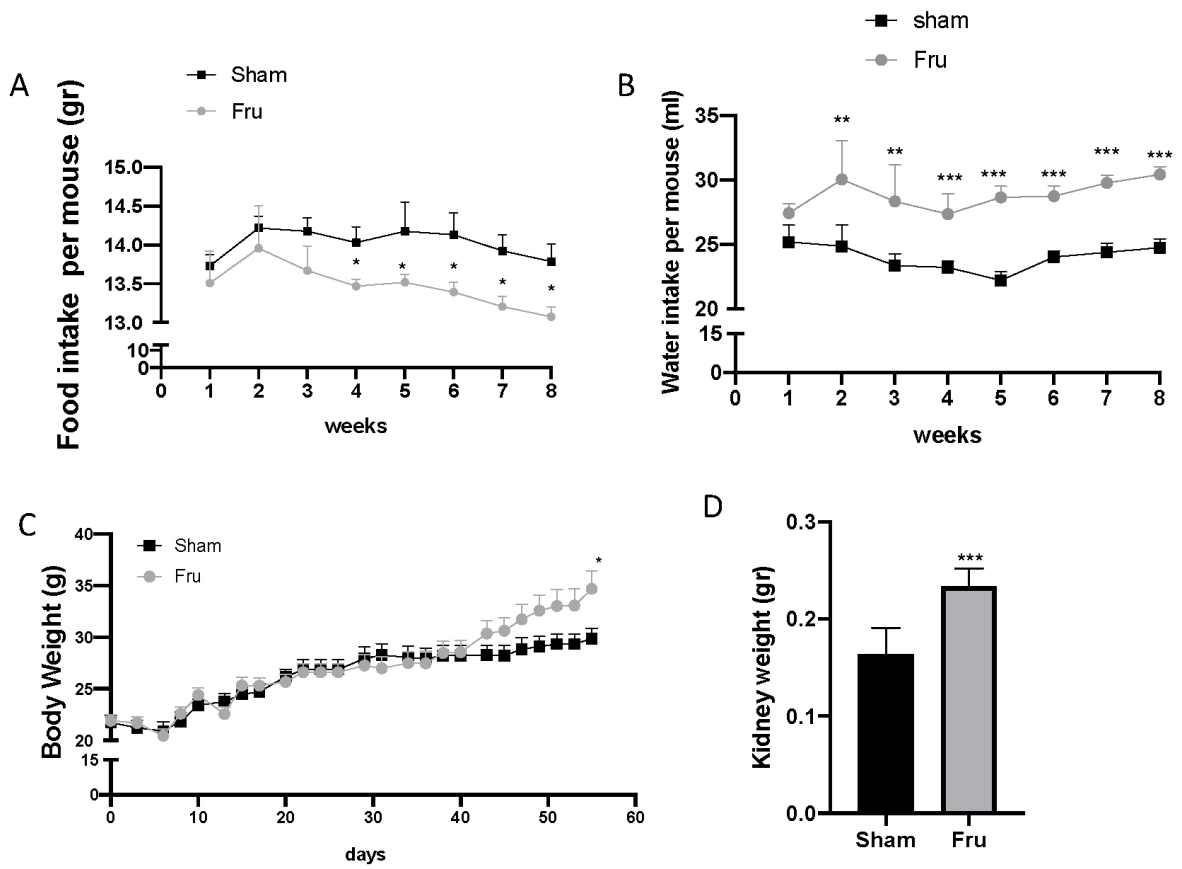

Fig. 1. Food intake (A), water intake (B), body weight (C), and kidney weight (D). (A,B) show mean daily food and water intake per mouse for every week. Data are presented as mean ± SEM of 6 animals/group. ***$p < 0.001$ vs. control, **$p < 0.01$ vs. control, *$p < 0.05$ vs. control. SEM, the mean standard error of the mean; Sham, Control group; Fru, Fructose group.

mogenized at the highest setting for 2 min; and centrifuged at 1000 *g* for 10 min at 4 °C. Supernatants represented the cytosolic fraction. The pellet, containing the nuclei, was resuspended in another buffer B containing protease inhibitors cocktail and 1% Triton X-100 (T8787, Sigma Aldrich, St., Louis, MO, USA); 150 mM NaCl (s9888, Sigma Aldrich, St., Louis, MO, USA); 10 mM Tris-HCl, pH 7.4; 1 mM EGTA; 1 mM EDTA. After centrifugation at 15,000 ×g for 30 min at 4 °C, the supernatant containing the nuclear protein were stored at –80 °C for further analysis. Protein concentration was estimated by the Bio-Rad protein assay (Bio-Rad, 5000006, Biogenerica SRL, CT, Italy) using bovine serum albumin (a9647, Sigma Aldrich, St., Louis, MO, USA) as standard. Samples were then heated at 95 °C for 5 min and equal amounts of protein separated on a 10–15% SDS-PAGE gel and transferred to a PVDF membrane (Immobilon-P ipvh00010, Biogenerica SRL, CT, Italy). Then, the filters were blocked with 1× PBS, 5% (w/v) nonfat dried milk for 40 min at room temperature and were subsequently probed with specific antibodies.

The following primary antibody was used: anti-OPN antibody (ab8448; Abcam, Milan, Italy), full-length OPN (which appears at 66 kDa) and -cleaved OPN (which appears at 32 kDa) incubated in 1× PBS, 5% (w/v) non-fat dried milk, 0.1% Tween-20 at +4 °C overnight. Membranes were then incubated with peroxidase-conjugated bovine anti-mouse IgG secondary antibody or peroxidase-conjugated goat anti-rabbit IgG 148901 (1:2000, Jackson ImmunoResearch, West Grove, PA, USA) for 1 h at room temperature. Anti β-actin antibody (1:5000, sc-47778, SCB, Biogenerica SRL, Catania, Italy) was used as the control. The expression of protein bands was detected as described [26].

Materials

All solutions used *in vivo* were prepared using nonpyrogenic saline (0.9% NaCl; 21385453, Baxter Healthcare Ltd., Thetford, Norfolk, UK).

Statistical Analysis

SEM = the mean standard error of the mean; N = the number of animals. The photos were from at least three different stainings/immunohistochemistry performed in different days. The data are expressed as mean ± SEM of N = 6 animals for each group. The results were analyzed by a non parametric Mann-Whitney U test $p < 0.05$ was considered significant.

Results

Food Intake, Water Consumption and Kidney and Body Weight

Food and water intake was checked throughout the experiment. Fructose mice consumed significantly more water than control mice during Weeks 2–8. The consumption of 30% fructose water was associated with significantly lower food intake than in controls from Weeks 4–8 ($p < 0.05$) (Fig. 1A), and ($p < 0.001$) and ($p < 0.01$) (Fig. 1B).

In addition, Fructose mice showed a significant increase in body weight at 56 days ($p < 0.05$) (Fig. 1C). Kidney weight was greater in the Fructose mice compared to control mice ($p < 0.001$) (Fig. 1D).

Clinical Biochemical Parameters Evaluation of Glucose and Lipid Metabolism and Liver Function of Fructose Mice

In the Fructose group, blood glucose was significantly higher than that of control group at all time points throughout the GTT ($p < 0.05$ and $p < 0.001$) (Fig. 2A). Glucose levels were significantly higher in Fructose mice compared to control group ($p < 0.001$) (Fig. 2B). Since MetS is also connected with lipid metabolism alterations [28], we analyzed the serum lipid profile at sacrifice. Fructose mice showed characteristics of hypertriglyceridemia, hypercholesteremia and a high level of LDL-C in serum compared to controls ($p < 0.001$) (Fig. 2C–E).

Additionally, levels of AST and ALT were significantly higher in Fructose mice than in control mice ($p < 0.001$) (Fig. 2F,G).

Clinical Biochemical Parameters Evaluation of Renal Function of Fructose Mice

Fructose mice had significantly higher serum BUN and creatinine concentration, as well as lower urinary creatinine levels compared to the control group ($p < 0.001$) (Fig. 2H–J).

Kidney Condition

Kidneys in the control group showed normal glomeruli and tubules (Fig. 3A,E). Kidneys of Fructose mice showed swelling in renal tubules, necrosis, and inflammatory infiltration ($p < 0.001$) (Fig. 3B,E) compared to the control group. Masson's trichrome staining showed that Fructose mice had more collagen mainly in the glomeruli and tubulointerstitium than the control mice ($p < 0.001$) (Fig. 3C,D,F).

Histological results indicated that Fructose mice had glomerular and fibrotic areas in the kidneys. The expression levels of TGF-β and α-SMA were significantly higher in Fructose mice than in control mice ($p < 0.001$) (Fig. 4A–F).

Evaluation of Osteopontin Levels

OPN levels were significantly higher in Fructose mice compared to controls ($p < 0.001$) (Fig. 5A). Increased gene and protein expression of OPN in kidney tissues in Fructose mice compared to controls ($p < 0.001$) (Fig. 5B,C,C1).

Discussion

MetS is a cluster of risk factors for heart disease, stroke, and type 2 diabetes [29,30]. Accredited organizations have continued their attempts to standardize the concept of MetS after the WHO panel issued its definition. However, different diagnostic standards are still applied in research [31]. When three or more risk factors, including abdominal obesity, high blood pressure, hypertriglyceridemia, hyperglycemia, and low levels of HDL cholesterol, are present, MetS is typically diagnosed [31]. In recent years, consuming fructose, primarily in the form of table sugar or high fructose corn syrup, has been linked to metabolic issues like insulin resistance and metabolic diseases [32,33]. Additionally, excessive fructose consumption has raised the mortality risk for renal disorders in both people and animals [34]. Due to its high lipogenicity, fructose can cause abnormalities in insulin signaling, dyslipidemia, aberrant glucose metabolism, hepatic steatosis, and renal dysfunctions [35–37]. The relationships of hyperuricemia and hyperhomocysteinemia with MetS contributed to renal function decline. Consuming fructose contributes to the development of CKD by increasing albuminuria and glomerular podocyte dysfunction [38]. Although significant advancements in diagnosis and therapy have been made, fructose-induced renal damage remains incurable. Hence, developing novel diagnosis biomarkers reflecting kidney damage is appealing for the timely diagnoses and therapy of MetS. OPN is a multi-functional cytokine and adhesion protein which is created in numerous tissues, including the kidney. OPN is expressed by a variety of cell types, including epithelial, mesenchymal, and hematopoietic cells including macrophages and T cells. OPN is produced in cultured kidney tubular epithelial, mesangial, and podocyte cells, and its expression is influenced by growth factors, cytokines, 1, 25(OH)2-vitamin D, and mechanical stress. Segments of the loop of Henle and the distal nephrons constitutively express OPN in the healthy kidney. OPN has been involved in several physiological and pathological events [39]. Based on these findings, this study helped to better understand whether OPM could be a biomarker of renal damage in experimental MetS. More research has shown that the inflammatory response plays a role in the renal damage caused by fructose in rodents [40,41]. Fructose and other metabolic stressors cause generalized inflammation, alter cell function, and cause pathologic changes in renal glomeruli and tubules [20]. Our data showed that mice administered 30% fructose via drinking water presented altered clinical biochem-

Journal of
BIOLOGICAL REGULATORS
and Homeostatic Agents

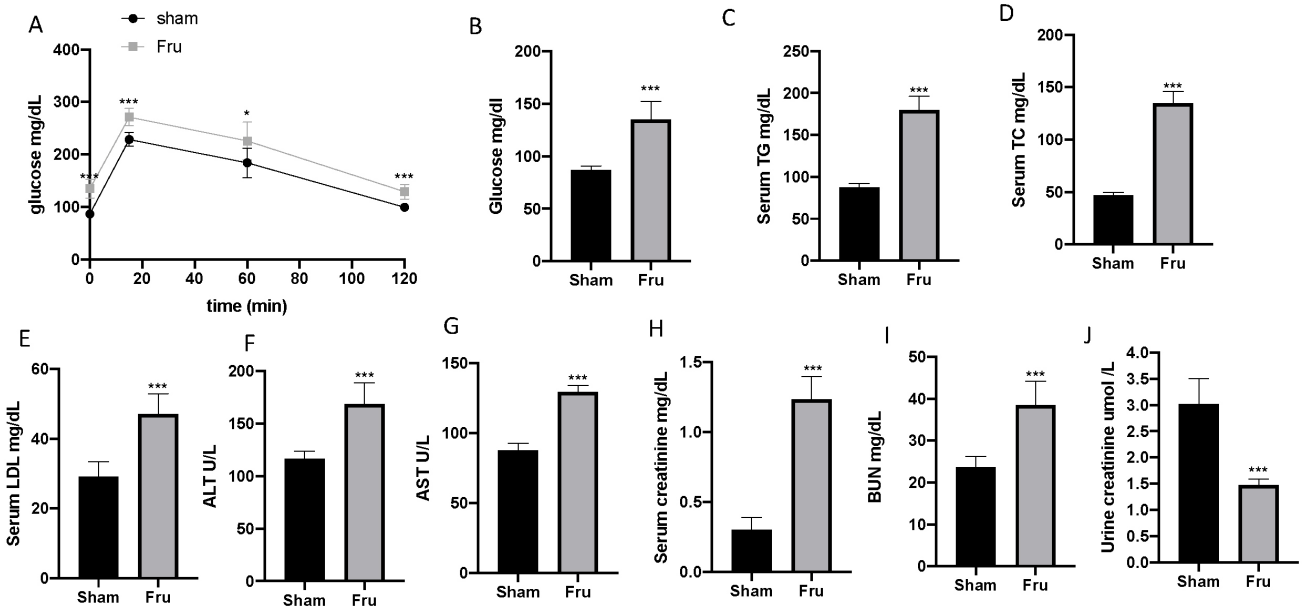

Fig. 2. Glucose Tolerance Test (A), Serum levels of glucose (B), TG (C), TC (D), LDL (E), ALT (F), AST (G), creatinine (H), BUN (I), urinary levels of creatinine (J). Data are presented as means ± SEM of 6 animals/group. ***$p < 0.001$ vs. control, *$p < 0.05$ vs. control. TC, total cholesterol; TG, triglyceride; LDL, low-density lipoprotein; ALT, alanine aminotransferase; AST, aspartate aminotransferase; BUN, blood urea nitrogen.

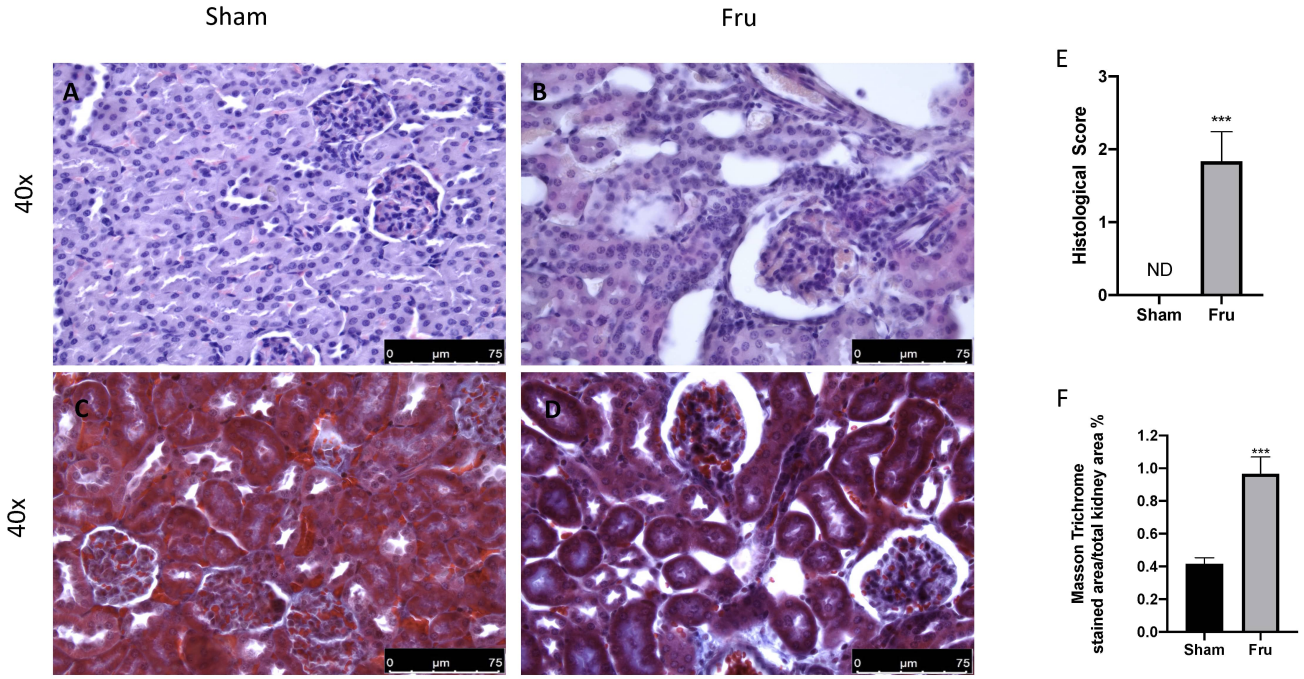

Fig. 3. Histological analysis. H&E staining of control (A), and Fructose mice (B), Masson Trichome staining of control (C), Fructose mice (D), histological score (E) and masson Trichome staining graph (F). Figures are representative of N = 3 independent stainings performed on different days. Data are presented as means ± SEM of 6 animals/group. Scale bar = 75 µm. Magnification 40×. ***$p < 0.001$ vs. control. H&E, haematoxylin and eosin; ND, not detected.

ical parameters of glucose metabolism, lipid profile, liver and renal function such as increased serum glucose, total cholesterol, triglyceride, low-density lipoprotein, alanine aminotransferase, and aspartate aminotransferase, as well as creatinine and blood urea nitrogen (BUN). Our results confirmed the status of MetS and related kidney function alterations. In addition, histological kidney injury and fibrosis were also observed. Several studies have proposed

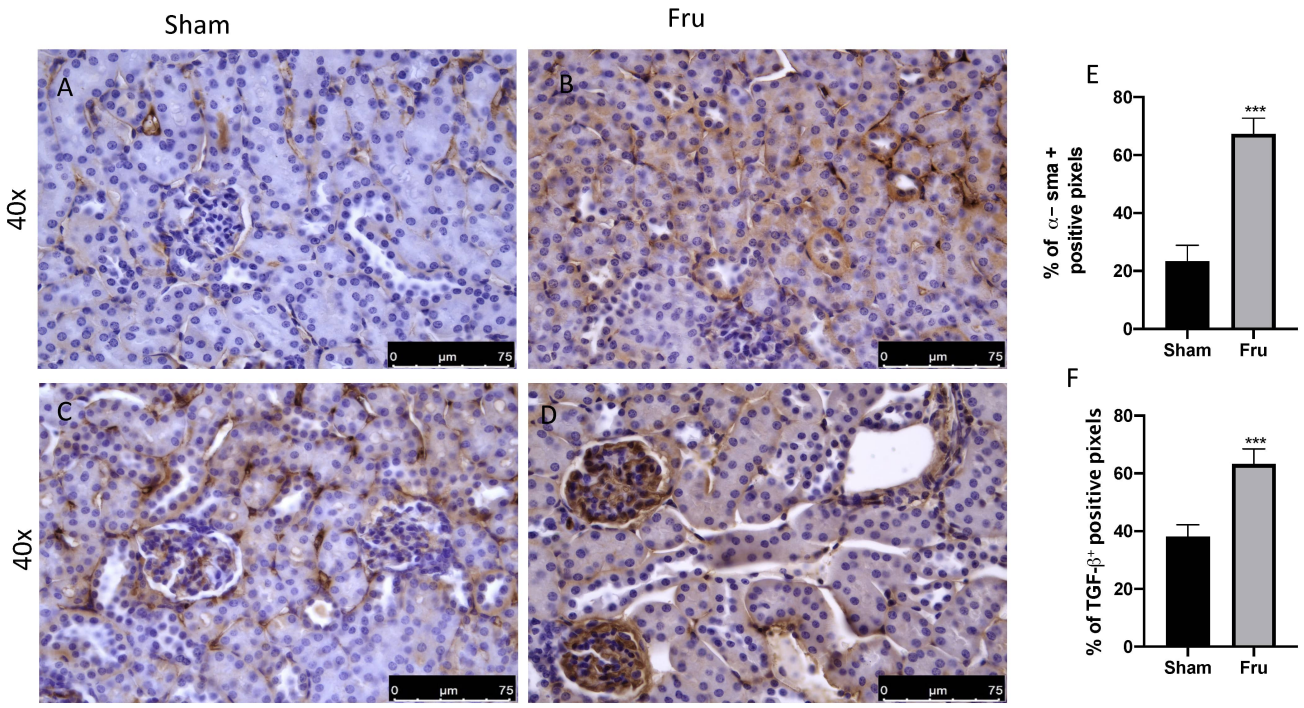

Fig. 4. Immunohistochemistry for α-SMA and TGF-β. Immunohistochemistry for α-SMA of control (A) and Fructose mice (B). Immunohistochemistry for TGF-β of control (C) and Fructose mice (D). The results are expressed as % of positive pixels (E,F). Figures are representative of N = 3 independent stainings performed on different days. Scale bar = 75 µm. Data are presented as mean ± SEM of 6 animals/group. Magnification 40×. ***$p < 0.001$ vs. control. α-SMA, Alpha Smooth Muscle Actin; TGF, Transforming Growth Factor.

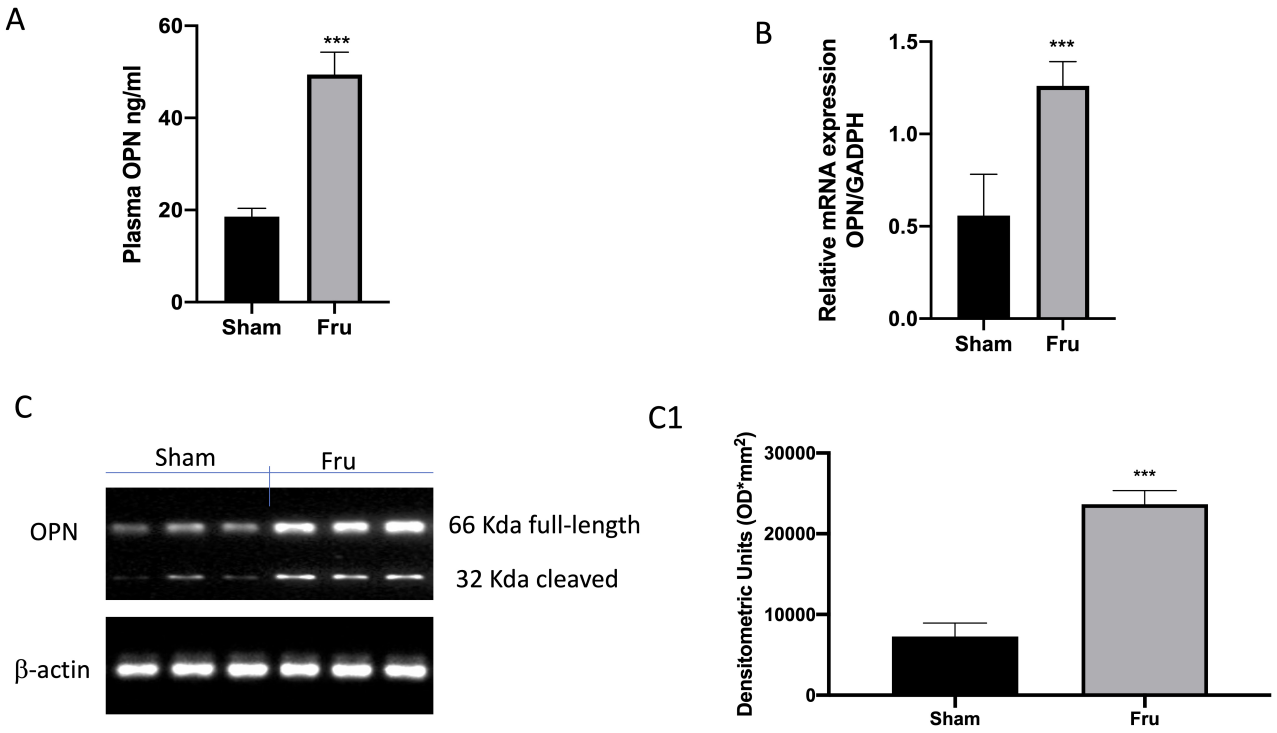

Fig. 5. OPN levels measurement. Plasma levels of OPN (A). Relative mRNA expression of OPN in kidney tissues (B). Western blot for OPN expression in kidney tissues (C). Exposed is a blot of lysates (6 animals/group) with a densitometric analysis for all animals (C1). Data are presented as mean ± SEM of 6 animals/group. ***$p < 0.001$ vs. control. OPN, osteopontin.

Journal of
BIOLOGICAL REGULATORS
and Homeostatic Agents

a possible profibrotic role for OPN [42]. After an acute ischemic insult, OPN promotes macrophage enrolment and increases the formation of renal scarring in kidney fibrosis [43,44]. Additionally, during myocardial infarction, OPN expression is elevated in the myocardium, and its absence is linked to a reduction in collagen accumulation [44]. Likewise, OPN seems to be a vital mediator of the cardiac profibrotic effects of angiotensin II by encouraging collagen synthesis and remodeling in the interstitial myocardium [45]. It has been proposed that OPN, which is generated by alveolar macrophages, works as a fibrogenic cytokine in experimental lung fibrosis [46]. The present study showed a significant increase in the interstitial collagen deposition in the Fructose group as demonstrated with Masson's trichrome. Aoyama *et al*. 2012 [47] also showed that rats fed with excess fructose presents tubulointerstitial fibrosis confined to the outer cortex of the kidney. The activated macrophages produce proinflammatory cytokines and TGF-β which may increase renal fibrosis [48]. A previous study also demonstrated that OPN in diabetic mice augments glomerular damage, through the expression of TGF-β [49]. In our study, Fructose mice had higher expression of α-SMA and TGF-β in the kidney, which coincides with increased collagen fibers. Similar results were obtained in other studies which showed increased α-SMA expression in the Fructose rat kidney [50]. Increased expression of OPN was found in several experimental models of renal injury [16,49,51]. Here, by PCR and western blot, we also demonstrated increased expression of OPN in renal tissues. In addition, serum levels of OPN as a biomarker, were measured in different experimental and clinical studies [52,53]. Patients with diabetes mellitus have an association between OPN plasma concentrations and the severity of nephropathy and coronary artery disease [54]. In this study we also found a significant increase of plasma OPN levels in Fructose mice as compared to control mice.

Limitation of Study

This study reported the identification of osteopontin as a biomarker to detect kidney damage induced by MetS. It is well known that this condition is also mainly associated to liver alteration. Here, we only measured serum levels of ALT and AST as markers of liver damage. Though both the liver and kidney have ALT and both the liver and heart muscle also have AST, more examination of the liver is needed.

Conclusions

In the clinical diagnosis and therapy, biomarkers which promote early identification, track the development of the disease, and provide follow-up prognosis are valuable. Early detection would give the opportunity to organize the proper surveillance and clinical management and make preventative measures more considerably efficient. This study represents a further confirmation that although not tissue specific, the level of OPN in association with conventional renal biomarkers can be considered for early diagnosis of kidney damage in patients with metabolic complications.

Availability of Data and Materials

All data included in this study are available upon request by contact with the corresponding author.

Author Contributions

All authors contributed to the study conception and design. The experiments were performed by AA, YM, RF, LI. Data collection and analysis were performed by RS, MC, GAF. The first draft of the manuscript was written by RD. Review and editing were performed by SC, RDP and DI. All authors contributed to editorial changes in the manuscript. All authors read and approved the final manuscript. All authors have participated sufficiently in the work and agreed to be accountable for all aspects of the work.

Ethics Approval and Consent to Participate

This study was approved by the University of Messina Review Board for the Care of Animals. The animal care conformed to the Italian regulations on the use of animals for experimental and scientific purposes (D.Lgs 2014/26 and EU Directive 2010/63). Ethical code: n.897/2021-PR.

Acknowledgment

We would like to thank Miss Valentina Malvagni for editorial support with the manuscript.

Funding

This research received no external funding.

Conflict of Interest

The authors declare no conflict of interest.

References

[1] Ahangarpour A, Mohammadian M, Dianat M. Antidiabetic effect of hydroalcholic urticadioica leaf extract in male rats with fructose-induced insulin resistance. Iranian Journal of Medical Sciences. 2012; 37: 181–186.

[2] Lin L, Tan W, Pan X, Tian E, Wu Z, Yang J. Metabolic Syndrome-Related Kidney Injury: A Review and Update. Frontiers in Endocrinology. 2022; 13: 904001.

[3] Flisiński M, Brymora A, Skoczylas-Makowska N, Stefańska A, Manitius J. Fructose-Rich Diet Is a Risk Factor for Metabolic Syndrome, Proximal Tubule Injury and Urolithiasis in Rats. International Journal of Molecular Sciences. 2021; 23: 203.

[4] Andres-Hernando A, Orlicky DJ, Cicerchi C, Kuwabara M, Garcia GE, Nakagawa T, *et al*. High Fructose Corn Syrup Ac-

celerates Kidney Disease and Mortality in Obese Mice with Metabolic Syndrome. Biomolecules. 2023; 13: 780.

[5] Srikanthan K, Feyh A, Visweshwar H, Shapiro JI, Sodhi K. Systematic Review of Metabolic Syndrome Biomarkers: A Panel for Early Detection, Management, and Risk Stratification in the West Virginian Population. International Journal of Medical Sciences. 2016; 13: 25–38.

[6] Sinha SK, Mellody M, Carpio MB, Damoiseaux R, Nicholas SB. Osteopontin as a Biomarker in Chronic Kidney Disease. Biomedicines. 2023; 11: 1356.

[7] Du Y, Mao L, Wang Z, Yan K, Zhang L, Zou J. Osteopontin - The stirring multifunctional regulatory factor in multisystem aging. Frontiers in Endocrinology. 2022; 13: 1014853.

[8] Kiss T, Jámbor K, Koroknai V, Szász I, Bárdos H, Mokánszki A, *et al*. Silencing Osteopontin Expression Inhibits Proliferation, Invasion and Induce Altered Protein Expression in Melanoma Cells. Pathology Oncology Research. 2021; 27: 581395.

[9] Tan Y, Zhao L, Yang YG, Liu W. The Role of Osteopontin in Tumor Progression Through Tumor-Associated Macrophages. Frontiers in Oncology. 2022; 12: 953283.

[10] Pagel CN, Wasgewatte Wijesinghe DK, Taghavi Esfandouni N, Mackie EJ. Osteopontin, inflammation and myogenesis: influencing regeneration, fibrosis and size of skeletal muscle. Journal of Cell Communication and Signaling. 2014; 8: 95–103.

[11] Lin EYH, Xi W, Aggarwal N, Shinohara ML. Osteopontin (OPN)/SPP1: from its biochemistry to biological functions in the innate immune system and the central nervous system (CNS). International Immunology. 2023; 35: 171–180.

[12] Si J, Wang C, Zhang D, Wang B, Zhou Y. Osteopontin in Bone Metabolism and Bone Diseases. Medical Science Monitor. 2020; 26: e919159.

[13] Cheng Y, Li Y, Scherer N, Grundner-Culemann F, Lehtimaki T, Mishra BH, *et al*. Genetics of osteopontin in patients with chronic kidney disease: The German Chronic Kidney Disease study. PLoS Genetics. 2022; 18: e1010139.

[14] Steinbrenner I, Sekula P, Kotsis F, von Cube M, Cheng Y, Nadal J, *et al*. Association of osteopontin with kidney function and kidney failure in chronic kidney disease patients: the GCKD study. Nephrology, Dialysis, Transplantation. 2023; 38: 1430–1438.

[15] Irita J, Okura T, Jotoku M, Nagao T, Enomoto D, Kurata M, *et al*. Osteopontin deficiency protects against aldosterone-induced inflammation, oxidative stress, and interstitial fibrosis in the kidney. American Journal of Physiology. Renal Physiology. 2011; 301: F833–F844.

[16] Zhang ZX, Shek K, Wang S, Huang X, Lau A, Yin Z, *et al*. Osteopontin expressed in tubular epithelial cells regulates NK cell-mediated kidney ischemia reperfusion injury. Journal of Immunology. 2010; 185: 967–973.

[17] Xu MX, Yu R, Shao LF, Zhang YX, Ge CX, Liu XM, *et al*. Up-regulated fractalkine (FKN) and its receptor CX3CR1 are involved in fructose-induced neuroinflammation: Suppression by curcumin. Brain, Behavior, and Immunity. 2016; 58: 69–81.

[18] Toda C, Kim JD, Impellizzeri D, Cuzzocrea S, Liu ZW, Diano S. UCP2 Regulates Mitochondrial Fission and Ventromedial Nucleus Control of Glucose Responsiveness. Cell. 2016; 164: 872–883.

[19] Chang CL, Sung PH, Chen KH, Shao PL, Yang CC, Cheng BC, *et al*. Adipose-derived mesenchymal stem cell-derived exosomes alleviate overwhelming systemic inflammatory reaction and organ damage and improve outcome in rat sepsis syndrome. American Journal of Translational Research. 2018; 10: 1053–1070.

[20] Yang M, Liu C, Jiang J, Zuo G, Lin X, Yamahara J, *et al*. Ginger extract diminishes chronic fructose consumption-induced kidney injury through suppression of renal overexpression of proinflammatory cytokines in rats. BMC Complementary and Alternative Medicine. 2014; 14: 174.

[21] Cordaro M, D'Amico R, Fusco R, Peritore AF, Genovese T, Interdonato L, *et al*. Discovering the Effects of Fisetin on NF-κB/NLRP-3/NRF-2 Molecular Pathways in a Mouse Model of Vascular Dementia Induced by Repeated Bilateral Carotid Occlusion. Biomedicines. 2022; 10: 1448.

[22] Di Paola R, Impellizzeri D, Mondello P, Velardi E, Aloisi C, Cappellani A, *et al*. Palmitoylethanolamide reduces early renal dysfunction and injury caused by experimental ischemia and reperfusion in mice. Shock. 2012; 38: 356–366.

[23] D'Amico R, Cordaro M, Fusco R, Peritore AF, Genovese T, Gugliandolo E, *et al*. Consumption of Cashew (*Anacardium occidentale* L.) Nuts Counteracts Oxidative Stress and Tissue Inflammation in Mild Hyperhomocysteinemia in Rats. Nutrients. 2022; 14: 1474.

[24] Impellizzeri D, Bruschetta G, Ahmad A, Crupi R, Siracusa R, Di Paola R, *et al*. Effects of palmitoylethanolamide and silymarin combination treatment in an animal model of kidney ischemia and reperfusion. European Journal of Pharmacology. 2015; 762: 136–149.

[25] Cordaro M, Siracusa R, Fusco R, D'Amico R, Peritore AF, Gugliandolo E, *et al*. Cashew (*Anacardium occidentale* L.) Nuts Counteract Oxidative Stress and Inflammation in an Acute Experimental Model of Carrageenan-Induced Paw Edema. Antioxidants. 2020; 9: 660.

[26] Siracusa R, D'Amico R, Cordaro M, Peritore AF, Genovese T, Gugliandolo E, *et al*. The Methyl Ester of 2-Cyano-3,12-Dioxooleana-1,9-Dien-28-Oic Acid Reduces Endometrial Lesions Development by Modulating the NFkB and Nrf2 Pathways. International Journal of Molecular Sciences. 2021; 22: 3991.

[27] Siracusa R, Paterniti I, Impellizzeri D, Cordaro M, Crupi R, Navarra M, *et al*. The Association of Palmitoylethanolamide with Luteolin Decreases Neuroinflammation and Stimulates Autophagy in Parkinson's Disease Model. CNS & Neurological Disorders Drug Targets. 2015; 14: 1350–1365.

[28] Yang M, Jiang ZH, Li CG, Zhu YJ, Li Z, Tang YZ, *et al*. Apigenin prevents metabolic syndrome in high-fructose diet-fed mice by Keap1-Nrf2 pathway. Biomedicine & Pharmacotherapy. 2018; 105: 1283–1290.

[29] Nakagawa T, Johnson RJ, Andres-Hernando A, Roncal-Jimenez C, Sanchez-Lozada LG, Tolan DR, *et al*. Fructose Production and Metabolism in the Kidney. Journal of the American Society of Nephrology. 2020; 31: 898–906.

[30] Hayden MR. Overview and New Insights into the Metabolic Syndrome: Risk Factors and Emerging Variables in the Development of Type 2 Diabetes and Cerebrocardiovascular Disease. Medicina. 2023; 59: 561.

[31] Cho Y, Lee SY. Useful Biomarkers of Metabolic Syndrome. International Journal of Environmental Research and Public Health. 2022; 19: 15003.

[32] Delbridge LMD, Benson VL, Ritchie RH, Mellor KM. Diabetic Cardiomyopathy: The Case for a Role of Fructose in Disease Etiology. Diabetes. 2016; 65: 3521–3528.

[33] Lozano I, Van der Werf R, Bietiger W, Seyfritz E, Peronet C, Pinget M, *et al*. High-fructose and high-fat diet-induced disorders in rats: impact on diabetes risk, hepatic and vascular complications. Nutrition & Metabolism. 2016; 13: 15.

[34] García-Arroyo FE, Gonzaga G, Muñoz-Jiménez I, Osorio-Alonso H, Iroz A, Vecchio M, *et al*. Antioxidant supplements as a novel mean for blocking recurrent heat stress-induced kidney damage following rehydration with fructose-containing beverages. Free Radical Biology & Medicine. 2019; 141: 182–191.

[35] Ajiboye TO, Hussaini AA, Nafiu BY, Ibitoye OB. Aqueous seed extract of Hunteria umbellata (K. Schum.) Hallier f. (Apocynaceae) palliates hyperglycemia, insulin resistance, dyslipi-

demia, inflammation and oxidative stress in high-fructose diet-induced metabolic syndrome in rats. Journal of Ethnopharmacology. 2017; 198: 184–193.

[36] Softic S, Cohen DE, Kahn CR. Role of Dietary Fructose and Hepatic De Novo Lipogenesis in Fatty Liver Disease. Digestive Diseases and Sciences. 2016; 61: 1282–1293.

[37] Toyoda K, Suzuki Y, Muta K, Masuyama T, Kakimoto K, Kobayashi A, *et al*. High fructose diet feeding accelerates diabetic nephropathy in Spontaneously Diabetic Torii (SDT) rats. The Journal of Toxicological Sciences. 2018; 43: 45–58.

[38] Bjornstad P, Lanaspa MA, Ishimoto T, Kosugi T, Kume S, Jalal D, *et al*. Fructose and uric acid in diabetic nephropathy. Diabetologia. 2015; 58: 1993–2002.

[39] Trostel J, Truong LD, Roncal-Jimenez C, Miyazaki M, Miyazaki-Anzai S, Kuwabara M, *et al*. Different effects of global osteopontin and macrophage osteopontin in glomerular injury. American Journal of Physiology. Renal Physiology. 2018; 315: F759–F768.

[40] Li Q, Xu Q, Tan J, Hu L, Ge C, Xu M. Carminic acid supplementation protects against fructose-induced kidney injury mainly through suppressing inflammation and oxidative stress via improving Nrf-2 signaling. Aging. 2021; 13: 10326–10353.

[41] Shen J, Yang X, Meng Z, Guo C. Protodioscin ameliorates fructose-induced renal injury via inhibition of the mitogen activated protein kinase pathway. Phytomedicine. 2016; 23: 1504–1510.

[42] Tang Z, Xia Z, Wang X, Liu Y. The critical role of osteopontin (OPN) in fibrotic diseases. Cytokine & Growth Factor Reviews. 2023. (online ahead of print)

[43] Vianello E, Kalousová M, Dozio E, Tacchini L, Zima T, Corsi Romanelli MM. Osteopontin: The Molecular Bridge between Fat and Cardiac-Renal Disorders. International Journal of Molecular Sciences. 2020; 21: 5568.

[44] Coculescu BI, Manole G, Dincă GV, Coculescu EC, Berteanu C, Stocheci CM. Osteopontin - a biomarker of disease, but also of stage stratification of the functional myocardial contractile deficit by chronic ischaemic heart disease. Journal of Enzyme Inhibition and Medicinal Chemistry. 2019; 34: 783–788.

[45] Abdelaziz Mohamed I, Gadeau AP, Hasan A, Abdulrahman N, Mraiche F. Osteopontin: A Promising Therapeutic Target in Cardiac Fibrosis. Cells. 2019; 8: 1558.

[46] Hatipoglu OF, Uctepe E, Opoku G, Wake H, Ikemura K, Ohtsuki T, *et al*. Osteopontin silencing attenuates bleomycin-induced murine pulmonary fibrosis by regulating epithelial-mesenchymal transition. Biomedicine & Pharmacotherapy. 2021; 139: 111633.

[47] Aoyama M, Isshiki K, Kume S, Chin-Kanasaki M, Araki H, Araki SI, *et al*. Fructose induces tubulointerstitial injury in the kidney of mice. Biochemical and Biophysical Research Communications. 2012; 419: 244–249.

[48] Wang X, Chen J, Xu J, Xie J, Harris DCH, Zheng G. The Role of Macrophages in Kidney Fibrosis. Frontiers in Physiology. 2021; 12: 705838.

[49] Nicholas SB, Liu J, Kim J, Ren Y, Collins AR, Nguyen L, *et al*. Critical role for osteopontin in diabetic nephropathy. Kidney International. 2010; 77: 588–600.

[50] Nakayama T, Kosugi T, Gersch M, Connor T, Sanchez-Lozada LG, Lanaspa MA, *et al*. Dietary fructose causes tubulointerstitial injury in the normal rat kidney. American Journal of Physiology. Renal Physiology. 2010; 298: F712–F720.

[51] Ophascharoensuk V, Giachelli CM, Gordon K, Hughes J, Pichler R, Brown P, *et al*. Obstructive uropathy in the mouse: role of osteopontin in interstitial fibrosis and apoptosis. Kidney International. 1999; 56: 571–580.

[52] Pereira TA, Syn WK, Pereira FEL, Lambertucci JR, Secor WE, Diehl AM. Serum osteopontin is a biomarker of severe fibrosis and portal hypertension in human and murine schistosomiasis mansoni. International Journal for Parasitology. 2016; 46: 829–832.

[53] Gao N, Zhang-Brotzge X, Wali B, Sayeed I, Chern JJ, Blackwell LS, *et al*. Plasma osteopontin may predict neuroinflammation and the severity of pediatric traumatic brain injury. Journal of Cerebral Blood Flow and Metabolism. 2020; 40: 35–43.

[54] Yan X, Sano M, Lu L, Wang W, Zhang Q, Zhang R, *et al*. Plasma concentrations of osteopontin, but not thrombin-cleaved osteopontin, are associated with the presence and severity of nephropathy and coronary artery disease in patients with type 2 diabetes mellitus. Cardiovascular Diabetology. 2010; 9: 70.